DIRECT MEASUREMENT OF PHASE SPACE EVOLUTION IN THE SPARC HIGH BRIGHTNESS PHOTOINJECTOR*

E. Chiadroni[a†], D. Alesini[a], A. Bacci[c], M. Bellaveglia[a], R. Boni[a], M. Boscolo[a], M. Castellano[a], L. Catani[b], S. Cialdi[c], A. Cianchi[b], A. Clozza[a], L. Cultrera[a], G. Di Pirro[a], A. Drago[a], A. Esposito[a], M. Ferrario[a], L. Ficcadenti[e], D. Filippetto[a], V. Fusco[a], A. Gallo[a], G. Gatti[a], A. Ghigo[a], L. Giannessi[d], M. Incurvati[a], C. Ligi[a], M. Migliorati[e], A. Mostacci[e], P. Musumeci[f], E. Pace[a], L. Palumbo[e], L. Pellegrino[a], M. Petrarca[g], M. Quattromini[d], R. Ricci[a], C. Ronsivalle[d], J. Rosenzweig[f], A.R. Rossi[c], C. Sanelli[a], L. Serafini[c], M. Serio[a], F. Sgamma[a], B. Spataro[a], F. Tazzioli[a], S. Tomassini[a], C. Vaccarezza[a], S. Vescovi[a], C. Vicario[a]

[a]INFN-LNF, via E. Fermi, 40 - 00044 Frascati, Rome, Italy

[b]INFN-Roma "Tor Vergata", via della Ricerca Scientifica, 1 - 00133 Rome, Italy

[c]INFN-Milano, Via Celoria 16, 20133 Milan, Italy

[d]ENEA C.R., via E. Fermi, 00044 Frascati, Rome, Italy

[e]Università di Roma "La Sapienza", Dip. Energetica, via A. Scarpa, 14 - 00161, Rome, Italy

[f]UCLA - Dept. of Physics and Astronomy, 405 Hilgard Avenue, Los Angeles, California 90095, USA

[g]INFN-Roma I, p.le A. Moro 5, 00185 Roma, Italy

Abstract

The characterization of the transverse phase space for high charge density relativistic electron beams is a fundamental requirement in many particle accelerator facilities, in particular those devoted to fourth-generation synchrotron radiation sources, such as SASE FEL.
The main purpose of the SPARC initial phase was the commissioning of the RF photoinjector. At this regard, the evolution of the phase space has been fully characterized by means of the emittance meter diagnostics tool, placed in the drift after the gun exit.
The large amount of collected data has allowed for the first time a detailed reconstruction of the transverse phase space evolution downstream the RF, giving evidences of the emittance compensation process as predicted by theory and simulations.
In particular the peculiar behavior of a flat top longitudinal electron distribution compared to a gaussian distribution has been studied giving important insights for the correct matching with the following linac whose working point is based on the double emittance minimum effect.

INTRODUCTION

The SPARC project is an R&D activity oriented to the development of a high brightness photoinjector to drive SASE FEL experiments [1]. In the first phase, the SPARC layout (Fig.1) consisted of a 1.6 cell RF gun operated at S-band (2.856 GHz, of the BNL/SLAC/UCLA type) and high peak field on the cathode ($\simeq$ 120 MV/m) with incorporated Copper photo-cathode, generating a 5.6 MeV energy beam. The first few meters of beam propagation, where space charge effects and plasma oscillations dominate the electron dynamics, have been studied by means of the movable emittance meter [2]. This device, based on the 1D

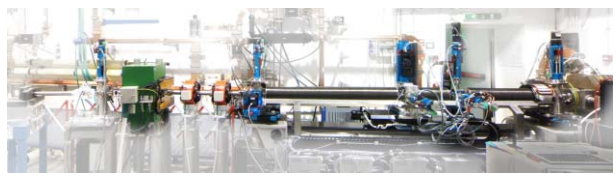

Figure 1: The SPARC photoinjector in the initial phase: from the right to the left, the RF gun with the solenoid, the emittance meter, quadrupoles and dipole magnets, the energy spectrometer and the beam dump.

pepper-pot technique, has allowed not only to measure the beam size and emittance, but also to reconstruct the transverse phase space at different positions along the direction of motion. Due to the high sensitivity of this method, a very precise emittance value can be calculated directly from the phase space analysis. For this reason, suitable data processing algorithms have been developed.
In the next phase of SPARC, which will start in Autumn, the beam emerging from the gun will be focused and matched into 3 accelerating sections of the SLAC type (S-band, TW), to boost the beam energy up to 155-200 MeV and to drive a SASE FEL at 530 nm.

SYSTEM DESCRIPTION AND OPTIMIZATION

To reach its goal SPARC requires a temporally flat, pico-second laser source. This source [3] is based on a Ti:sapphire oscillator that generates 100 fs pulses with a

* Work partially supported by the EU Commission in the sixth framework program, Contract No. 011935 EUROFEL-DS1 and from the MIUR Progetti Strategici DD1834.

† enrica.chiadroni@lnf.infn.it

repetition rate of 79.33 MHz locked with the 36^{th} subharmonic of the SPARC S-band master clock. The measured time jitter is within 1 ps. An acousto-optic dispersive filter, called DAZZLER, is placed between the oscillator and the amplifier to modify the spectral amplitude and phase function to obtain the target temporal profile [4]. The amplifier delivers pulses at 800 nm with energy of 50 mJ and a repetition rate of 10 Hz. The pulses go to the third harmonic generator and UV pulses at 266 nm are produced. At the end of the laser chain there is a grating stretcher to stretch the pulses temporally up to 8-12 ps [5]. After that the optical transfer line transports the laser beam at normal incidence to the cathode with an energy between 50 and 100 μJ.

Since the uniformity of the transverse distribution strongly influences the beam brightness, a dedicated laser cleaning has been performed with 10 μJ and 100 μm spot size diameter, resulting in the increase of the mean quantum efficiency (QE) from 2.3 10^{-5} to 10^{-4} (Fig.2). An improvement of the emission uniformity has been found over a 4 mm square area, which allowed to get the nominal beam parameters (1 nC electron beam charge, with 50 μJ laser pulse energy at 120 MV/m peak field on the cathode).

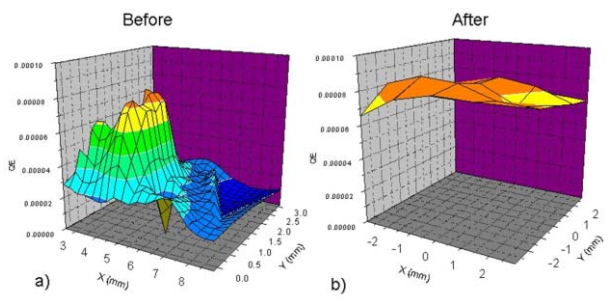

Figure 2: Copper cathode quantum efficiency before (left) and after (right) the laser cleaning.

The Emittance Meter

At the gun exit the beam is quasi-relativistic and conventional methods to measure the transverse emittance are not adequate due to the fact that internal collective forces play a fundamental role in the beam transport. For such space charge dominated beams, the most appropriate technique to measure RMS (root mean square) transverse emittance is the one based on the pepper pot method. This technique, which consists in splitting the beam into several beamlets by means of a multislit mask intercepting the beam or, alternatively, a single slit moving across the beam spot, is implemented in a device, called emittance meter, able to scan the 2 meters long region downstream the gun along the beam line. The emittance can be measured in both x and y planes at different positions along the direction of beam propagation in the range 1098 - 2100 mm following the emittance oscillations. In particular, due to the high measurement resolution, the entire distribution in space and angles can be precisely reconstructed from the sampling in both directions, allowing the full characterization of the beam transverse dynamics.

The complete knowledge of the beam parameters at different distances from the cathode is important also for defining the injector settings which optimize the emittance compensation process and for code validation.

Beyond a transverse diagnostics, the emittance meter allows also to get information on the beam longitudinal parameters. By selecting the central part of the beam with a slit, the evolution of the energy spread can be measured at different z positions. The very good agreement between measurements and PARMELA model, which does not take into account the wake-fields effect, points out that the influence of the long emittance meter bellows is negligible (Fig.3).

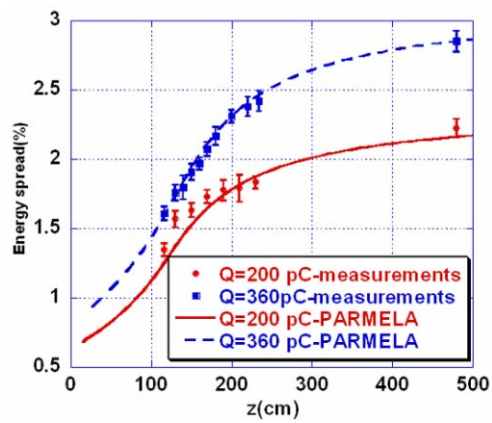

Figure 3: Evolution of the energy spread versus z for two different bunch charges compared with a PARMELA simulation.

DATA ANALYSIS

For the first time direct emittance evolution measurements and experimental studies of dynamical behavior have been done.

Since the beam appears different during its propagation along z, the estimation of the right beam halos and the preservation of the same cut level at different locations are critical issues to deal with. Indeed, conventional image processing tools might introduce artifacts which could cover small fluctuations in the beam emittance dynamics.

Furthermore, the large amount of data collected has demanded the development of an automatic procedure for data processing. At this purpose, three independent algorithms, based on different approaches, have been developed for the emittance calculations: i) a single image analysis and data extrapolation [6], ii) a trace space plot filtering [7] and iii) a genetic-based algorithm [8].

Single Image Analysis and Data Extrapolation

The main program data flow is shown in Fig.4. It consists of four routines.

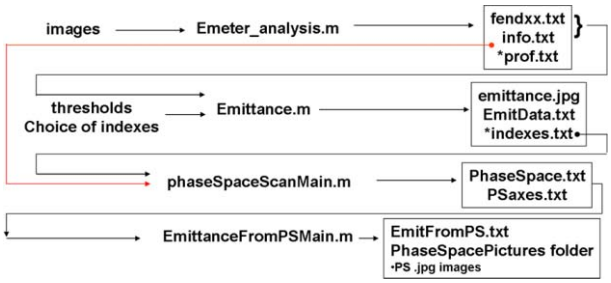

Figure 4: The analysis software data flow. The central column corresponds to the routine names, the left one shows the input parameters while the right one the output parameters.

The first one is the core of the algorithm oriented to distinguish the signal from noise; it takes raw beamlets images as input and after processing their profiles it calculates from them the moments of the beamlet charge distribution, i.e. beamlet area, centroid and rms width along the direction perpendicular to slit edges.
The second routine takes as input the files saved by the first one, cleans data from bad values and calculates the emittance in two different ways: i) by averaging slit parameters and/or ii) by averaging different emittances calculated from each single parameter. The third routine reconstructs and saves the trace space for each single emittance measurement and the fourth one interpolates the trace space in order to have more sampling along the abscissa and then calculates the emittance from the trace space with the desired cut in charge.
This analysis procedure automatically operates a cut on the charge effectively considered in the emittance computation, whose level cannot be trivially retrieved. For this reason and to validate and support the data analysis method, two more algorithms have been developed, both starting from the transverse phase spaces.

Phase Space Filtering

The goals of this code are the calculation of the emittance value directly from the phase space data and the quantification of the cut level introduced on the beam by the previous algorithm.
The idea is to quantify the contribution of every pixel to the total emittance, retrieving the value of the x, x' and using it in the Courant-Snyder invariant to calculate the emittance. The emittance can then be used as sorting parameter, so that pixels with the highest contribution on the emittance value, probably outside the beam core, are withdrawn.
Starting from these pixels the total charge and the second derivative of the emittance with respect to the charge is calculated. A phenomenological evidence has shown a deep, sharp peak in the second derivative in all the reconstructed trace spaces.
Montecarlo simulations have demonstrated that this peak appears in the transition between signal and noise, if the signal-to-noise ratio and the speed of the signal increment over the noisy background are high enough. Assuming this point to be 100% of the beam charge, it is possible to define an emittance value depending on the charge cut level.

Genetic Algorithm

The basic concept relies on the fact that a real beam can be thought as composed by N sub-beams of different densities drawing concentric ellipses in the trace space, with different slopes and covering areas of different intensities.
Starting from the interpolated phase space, the code generates an intensity distribution function from which the total intensity and the cut parameter are retrieved. Each ellipse is described by the three Twiss parameters and the trace space centroid by two coordinates. A family of N solutions, called chromosomes, is generated, each of which corresponding to 2+3N parameters. Therefore the best set of ellipses is found by maximizing the Intensity/Area function, the area corresponding to the beam geometric emittance.
The code is optimized for N=8, but it can accept any number of ellipses. Fig.5 shows a very good agreement between the genetic solution, given by the union of the eight analytical ellipses, and the projected distribution of the real bunch.

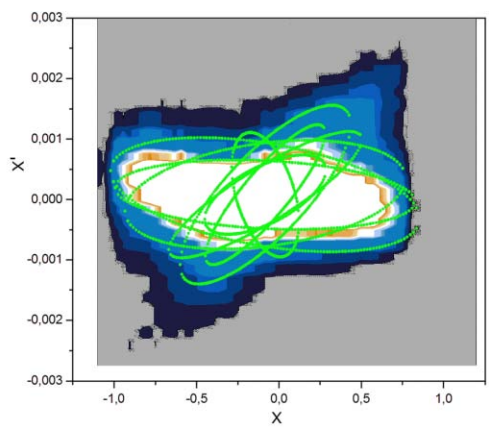

Figure 5: Real beam sampled with 8 ellipses representing the best chromosome.

Comparison

Many different emittance curves have been analyzed and here is shown one of the most significant to compare all the codes. Indeed, the small amplitude of the double minimum oscillation is an excellent candidate to check that every method is able to resolve it. Experimental data are compared in Fig.6 to a numerical fit with the PARMELA tracking code, showing a very good agreement [9].

The cutting level is 95% for the phase space algorithm and 97% for the genetic-based algorithm.

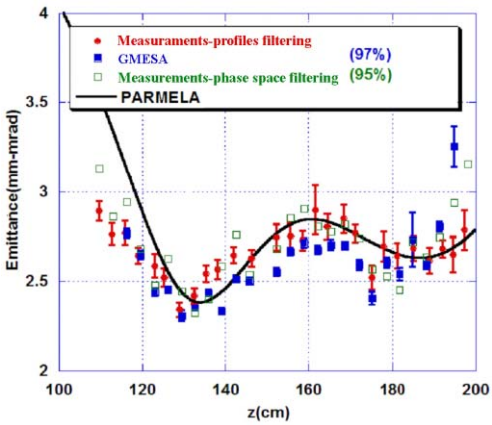

Figure 6: Comparison between different algorithms and PARMELA simulation.

RESULTS HIGHLIGHTS

Comparison between Gaussian and Flat-Top Pulse

An accurate study, supported by PARMELA simulations (Fig.7), has been done to show how the beam dynamics strongly depends on the laser pulse rise time. It is evident

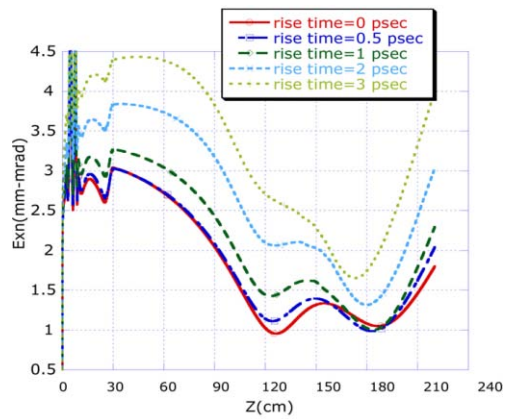

Figure 7: PARMELA simulation of the emittance evolution for pulses with different rise time.

that under the same conditions, the shortest rise time gives not only the smallest emittance minimum, but it makes also the double minimum oscillation more pronounced, whereas at longer rise time it turns into a knee.

Experimentally we compared two different pulse shapes with the same FWHM equals to 8.7 ps, but with different rise time: 5 ps for the Gaussian-like pulse and about 2.5 ps for the flat-top-like pulse (Fig.8a). The resulting emittance evolution in the vertical plane, for a beam of 0.31 mm rms spot size, 0.74 nC charge and 5.4 MeV energy, is shown in

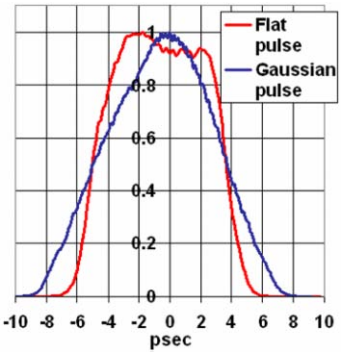

(a)

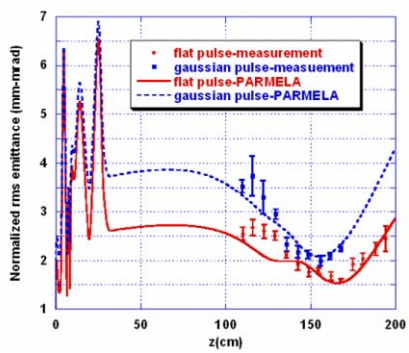

(b)

Figure 8: a) Gaussian-like and flat-top-like pulse shapes with the same FWHM = 8.7 ps. b) Measured emittance evolution of Gaussian and flat top beams compared with PARMELA simulations.

Fig.8b. The comparison points out that the minimum emittance value is reduced from 2 to 1.5 mm-mrad by using a flat-top shape instead of a gaussian pulse, accordingly with PARMELA simulations.

High Brightness Beam

A large number of runs were devoted to maximize the brightness by minimizing the transverse emittance. The best result, obtained with the flat-top longitudinal profile shown in Fig.9, is presented in Fig.10 [10]. The minimum

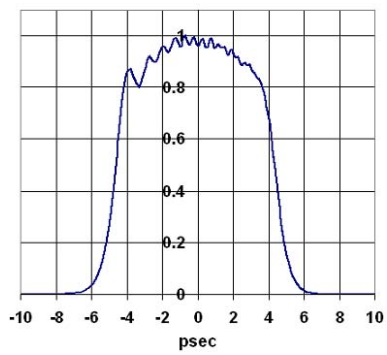

Figure 9: Laser pulse longitudinal profile: FWHM = 9 ps, rise time = 2.7 ps.

emittance, for a beam with peak current of 92 A, is 1.6 mm-mrad, giving a peak brightness of 7 10^{13} A/mm^2. The injection phase was set to -8 deg with respect to the maximum energy gain phase and the rms spot size was 360 μm. The simulation made with PARMELA (solid line in the plot of Fig.10) reveals a very good agreement with the experimental data.

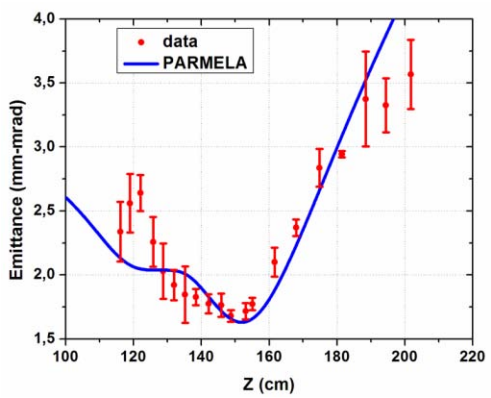

Figure 10: Emittance as function of the longitudinal coordinate for high brightness beam.

Double Minimum Signature

The peculiar space charge regime which, in the flat top pulse mode, gives rise to the emittance oscillation, observed up to now in numerical simulations only and on which photoinjectors worldwide have based the most common compensation design, has been revealed [11] by strongly reducing the rise time down to 1.5 ps (the longitudinal profile is shown in Fig.11) and moving the injection phase of 12 degrees behind the phase of maximum energy gain in order to increase the beam energy spread accordingly with the chromatic nature of the effect. The bunch

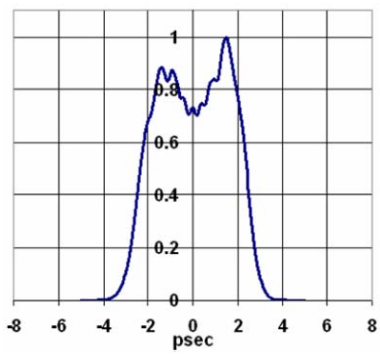

Figure 11: Laser pulse longitudinal profile: FWHM = 5 ps, rise time = 1.5 ps.

charge was 0.5 nC in a 5 ps FWHM laser pulse length, corresponding to 100 A peak current. The beam energy was 5.5 MeV.
The evolution of the emittance along z, in very good agreement with PARMELA simulations, is shown in Fig.12. The amplitude of the oscillation is about 0.3 μm which is above the resolution of our measurement system.

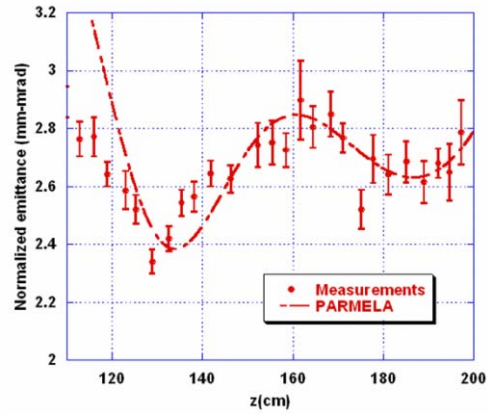

Figure 12: Double minimum emittance oscillation with corresponding PARMELA simulation.

Phase Space Analysis

Emittance oscillations have been explained as produced by a beating between head and tail particles oscillating with different plasma frequencies caused by correlated chromatic effects in the solenoid [12].
In the space charge dominated regime, simulations show a cross shape in the transverse phase space of a flat top distribution at its relative emittance maximum, corresponding to the beam waist (Fig.13b), due to the fact that each slice, which shapes the beam up, has the same weight in current. Thus, under laminar condition, the space charge dominated waist is reached at different positions by the head and the tail of the bunch (Fig.13b, left picture), so that when the bunch tail (green slice) is already diverging the bunch head (red slice) is still converging, resulting in the observed cross shaped transverse phase space.
In the Gaussian pulse case (Fig.13a), this effect is less pronounced since the amount of current at the bunch tails is smaller, thus causing the bunch tails to go through a crossover and only the central slices through a waist [13], [14].
A comparison of the transverse phase space at the beam waist as retrieved from beam measurements for both Gaussian and flat top distribution is reported in Fig.14. According to theory, experimental data show that a flat top beam goes through a space charge dominated waist passing from convergent to divergent, resulting in the typical cross shape in the reconstructed transverse phase space (Fig.14b), while it is absent in case of Gaussian beam (Fig.14a).

CONCLUSIONS

The initial phase of the SPARC project is concluded showing, for the first time experimentally and due to a movable diagnostics, the oscillation of the emittance in the region, downstream the RF gun, where the emittance com-

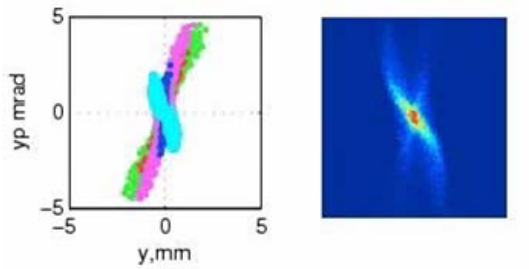

(a) Gaussian beam

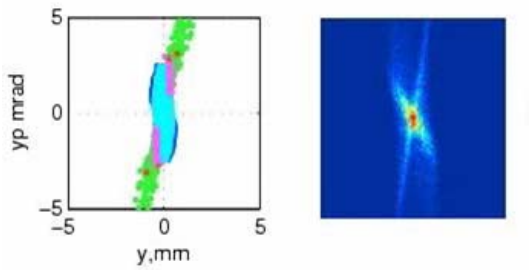

(b) Flat top beam

Figure 13: PARMELA simulation of the transverse phase space for a beam approaching its waist. Left pictures show the ensemble of slices shaping the beam up: green is the bunch tail, light blue the center of the bunch and red the head.

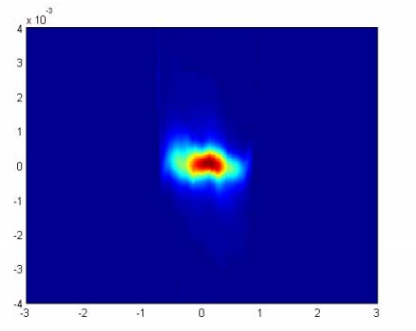

(a) Gaussian beam

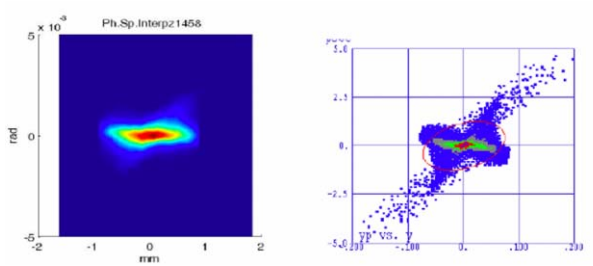

(b) Flat top beam

Figure 14: Reconstructed (left) transverse phase space at the beam waist compared with PARMELA simulation (right).

pensation process is predicted by theory. The high sensitivity of this diagnostics has allowed also to fully reconstruct the beam transverse phase space from which, due to the very high sampling rate, the emittance dynamics has been reproduced in excellent agreement with the simulation.
The large amount of data collected has required the development of automatic tools for data processing which gives a validation of measurement results, being all quantitatively consistent with simulations and with each other.

ACKNOWLEDGMENTS

The authors wish to thank V. Lollo for his contribution to the system mechanical design, engineering and bench testing, F. Anelli and S. Fioravanti for their work on motor controllers. Thanks also to A. Battisti, L. Cacciotti, L.A. Rossi, R. Sorchetti and S. Strabioli.

REFERENCES

[1] SPARC Project Team, Technical Design Report for the SPARC Advanced Photoinjector, http://www.lnf.infn.it/acceleratori/sparc (2004)

[2] L. Catani et al., Review of Scientific Instruments **77**, (2006) 93301.

[3] C. Vicario et al., "Drive Laser System for SPARC Photoinjector", Proceedings of the PAC'07, Albuquerque, NM, USA, June 2007.

[4] S. Cialdi et al., Optics Letters **31**, (2006) 2885.

[5] S. Cialdi et al., Applied Optics **46**, 22, (2007) 4959.

[6] D. Filippetto, "A robust algorithm for beam emittance and trace space evolution reconstruction", SPARC/EBD-07/002, LNF-INFN, June 2007.

[7] A. Cianchi et al., "Accurate emittance calculation from phase space analysis", SPARC/EBD-07/003, LNF-INFN, July 2007.

[8] A. Bacci et al., "A Genetic Code able to compute the emittance value of a real beam by a Multiple Ellipse Slice Analysis of the transversal phase-space image", SPARC/EBD-07/004, LNF-INFN, July 2007.

[9] C. Ronsivalle et al., "Comparison between SPARC e-meter measurements and simulations", Proceedings of the PAC'07, Albuquerque, NM, USA, June 2007.

[10] A. Cianchi et al., "High brightness electron beam emittance evolution measurements in SPARC RF photoinjector", submitted to Phys. Rev., ST-AB.

[11] M. Ferrario et al., "Direct measurement of double emittance minimum in the SPARC high brightness photoinjector", submitted to Physical Review Letters.

[12] M. Ferrario et al., "Recent Advances and Novel Ideas for High Brightness Electron Beam Production Based on Photo-Injectors", The Physics and Application of High Brightness Electron Beam (World Scientific Publishing Co. Pte. Ltd., 2002).

[13] B.E. Carlsten, Nucl. Instrum. & Methods A **285**, (1989) 313.

[14] L. Serafini, J.B. Rosenzweig, Phys. Rev. E **55** (1997) 7565.